Research Article

High-Performance Organic Flexible Thermoelectric Devices for Wearable Applications

Benjamin Wang

Portola High School, 1001 Cadence, Irvine, CA 92618, USA

ABSTRACT

In recent years, thermoelectric (TE) devices have garnered increasing attention for their ability to convert waste heat into usable electrical energy, offering a pathway toward enhanced energy efficiency and reduced carbon emissions. Among various TE technologies, flexible thermoelectric generators stand out as promising candidates for powering wearable electronics and industrial Internet of Things applications due to their lightweight, compact, and maintenance-free design. Unlike conventional rigid devices, these solid-state systems can conform to diverse heat sources, enabling seamless integration into both personal and industrial environments. Compared to inorganic materials, organic TE materials present compelling advantages for room-temperature and flexible energy harvesting. In this study, we investigate the thermoelectric performance of films composed of poly(3,4-ethylenedioxythiophene):poly(styrenesulfonate) blended with graphene nanoplatelets. The maximum power factor of ~12 ± 1.3 μW/mK^2 is achieved for unsintered films at room temperature. Additionally, an in-plane device prototype was developed, achieving a maximum open circuit voltage of 5.1 mV under a temperature gradient of 15 K. These findings underscore the potential of organic thermoelectric materials for next-generation flexible and wearable energy solutions.

Keywords: Organic thermoelectrics; energy harvesting; PEDOT:PSS; graphene; wearable applications

INTRODUCTION

Flexible thermoelectric generators (TEGs) have emerged as promising power sources for wearable electronics and Internet of Things (IoT) devices. These solid-state energy converters are lightweight, compact, and operate silently without any moving parts, offering a maintenance-free solution for energy harvesting. Recent advances in thermoelectric materials and device engineering have significantly enhanced their performance, enabling the development of next-generation TEGs. These systems provide environmentally friendly and mechanically simple means of converting heat directly into electricity, making them well-suited for a wide range of applications, from personal health monitors to industrial sensors (1-5).

Corresponding author: Benjamin Wang, E-mail: benjaminwang2078@gmail.com.

Received May 20, 2025**; Accepted** June 15, 2025
https://doi.org/10.70251/HYJR2348.33139146

Figure 1 shows a schematic of an in-plane thermoelectric device capable of directly converting temperature differences into electrical energy through the Seebeck effect. The Seebeck effect occurs when there is a temperature difference at the junction of two different semiconductors, enabling thermoelectric devices to effectively convert thermal energy into electrical energy. Additionally, these devices can utilize the Peltier effect, where an electric current passing through two different conductors at their junction causes one side to absorb heat while the other releases heat, creating a temperature gradient.

The efficiency of thermoelectric (TE) materials largely depends on the dimensionless figure of merit (zT) defined as $zT = \frac{\sigma S^2}{\kappa} T$ where S is the Seebeck coefficient, σ is the electrical conductivity, κ is the thermal conductivity, and T is the absolute temperature. The numerator of this relationship (σS^2) is known as Power Factor (PF). To increase the zT, it is needed to enhance the electrical properties of the TE materials including electrical conductivity and Seebeck coefficient, however, increasing these properties tends to also raise the thermal conductivity since they are interdependent. Thus, the challenge is to optimize TE properties to boost zT, balancing the need for TE materials with high electrical conductivity and low thermal conductivity (6, 7).

Thermoelectric materials can be broadly classified into organic and inorganic categories, each offering distinct advantages and limitations. Organic materials, although characterized by relatively low thermoelectric efficiency (zT values), are attractive due to their environmental friendliness, mechanical flexibility, and non-toxic nature. In contrast, inorganic materials typically exhibit higher zT values and superior performance but are often brittle, expensive, and potentially toxic, which restricts their applicability in flexible or wearable technologies. Ongoing research continues to focus on optimizing the trade-offs between these material classes to enhance the overall efficiency and usability of thermoelectric devices (8, 9).

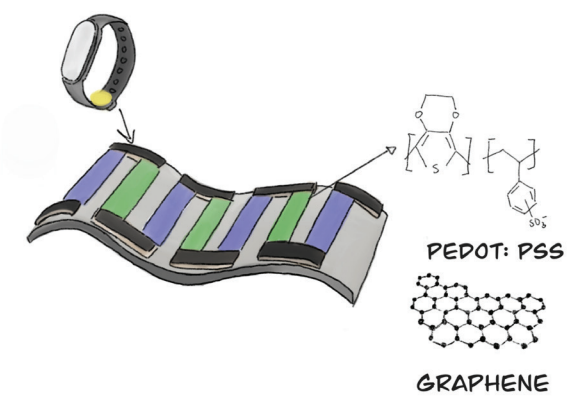

Figure 1. Schematic of an organic flexible thermoelectric device for energy harvesting using PEDOT:PSS and graphene nanoplatelets.

Recent studies on unsintered organic thermoelectric materials have demonstrated notable advances in power factor (PF), particularly through polymer composites and organic–inorganic hybrids. For example, P3HT/SWNT composites achieved power factors ranging from 107 $\mu W \cdot m^{-1} \cdot K^{-2}$ (10) to 308 $\mu W \cdot m^{-1} \cdot K^{-2}$ after $FeCl_3$ doping (11), and spray-printed versions reached 325 $\mu W \cdot m^{-1} \cdot K^{-2}$ (12). Gärisch et al. showed that layer-by-layer PEDOT:PSS/DWNT films doped with KBr yields a power factor of 626 $\mu W \cdot m^{-1} \cdot K^{-2}$ (13), while ionic-liquid-treated PEDOT:PSS reached 754 $\mu W \cdot m^{-1} \cdot K^{-2}$ (14). Se-substituted diketopyrrolopyrrole polymers (PDPPSe-12) showed PFs from 300 to 364 $\mu W \cdot m^{-1} \cdot K^{-2}$ (15). A TiS_2-based n-type organic–inorganic superlattice exhibited PF up to 904 $\mu W \cdot m^{-1} \cdot K^{-2}$ (16). The highest reported PF among these systems is 1825 $\mu W \cdot m^{-1} \cdot K^{-2}$ in a PANI/graphene/DWNT nanocomposite (17), demonstrating the impressive potential of hybrid architectures for high-performance flexible thermoelectrics.

Among organic materials, poly(3,4-ethylenedioxythiophene) polystyrene sulfonate knows as PEDOT:PSS has received tremendous attention due to its high electrical properties and aspect ratio. PEDOT:PSS is a blend of two distinct polymers—poly(3,4-ethylenedioxythiophene) (PEDOT) and polystyrene sulfonate (PSS). PEDOT is a semiconductor known for its high electrical conductivity and ease of processability, while PSS provides stability and enables water dispersion, making PEDOT:PSS a versatile material for various applications. PEDOT offers impressive mechanical flexibility and conductivity, while PSS enhances stability and performance. Combining these materials results in a transparent substance in the visible spectrum (18, 19).

During the synthesis of PEDOT:PSS, PEDOT forms on a PSS template, and small segments of PEDOT come into close contact with PSS bundles, bound by Coulomb forces. This results in chain structure entanglement and colloidal gel particles in water, contributing to its unique properties. The high electrical conductivity of PEDOT stems from its molecular structure, which allows free electron movement through the polymer chain. In terms of thermoelectric performance, PEDOT has high electrical and low thermal conductivity, making it an ideal candidate for thermoelectric applications. In addition, this

combination makes PEDOT:PSS an excellent candidate for other applications including optical and electronic devices. Moreover, PEDOT:PSS offers several advantages such as high mechanical flexibility, low surface roughness, and low cost compared to other conjugated polymers (20).

Graphene is a two-dimensional material, a single layer of carbon atoms arranged in a hexagonal lattice, known for its exceptional strength, flexibility, and conductivity, making it a promising material for various applications (21). Since the discovery of graphene in 2004, it has been used for a variety of applications including electronics, sensing, optics, bioengineering, etc. (22, 23). The bond length of graphene is 0.142 nm, and when layers of graphene are stacked together, they form graphite, which has an interplanar spacing of 0.335 nm. The individual graphene layers in graphite are held together by Van der Waals forces, which can be overcome during the exfoliation process to obtain pure graphene (24).

Graphene is lightweight, highly flexible, and stable under high temperatures. Its unique structure allows charge carriers to move through it easily, making it an excellent thermoelectric material. Graphene can absorb significant amounts of heat, making it suitable for converting thermal energy into electrical power. Additionally, graphene exhibits high electrical conductivity, making it highly advantageous for energy conversion applications (25). As carbon is the second most abundant element in the human body and the fourth most abundant in the universe, graphene presents an eco-friendly and sustainable solution for thermoelectric energy conversion. Beyond its thermoelectric capabilities, graphene is also used to enhance the capacity, charging rate, and longevity of batteries. In this work, we studied the TE properties of films made of PEDOT:PSS blended with graphene and the impact of sintering on thermoelectric performance. Sintering plays a critical role in thermoelectric material processing by enhancing electrical conductivity and mechanical integrity through improved particle bonding and densification. By promoting better grain connectivity and reducing interfacial resistance, sintering can significantly improve charge carrier mobility and overall transport properties. However, the process must be carefully optimized, especially for organic or hybrid materials, to avoid degradation or loss of functional properties due to excessive heat exposure. Sintering transforms TE particles into a dense structure with improved thermoelectric properties. The unsintered films showed a Seebeck coefficient and an electrical conductivity of -71 ± 2.9 μV/K and 2373.3 ± 160.8 S/m, respectively. This led to a power factor of ~12 ± 1.3 μW/mK^2. This study exhibited the role of organic TE devices for integration with low-grade electronics and wearable applications.

METHODS AND MATERIALS

Thermoelectric films made using vacuum-assisted filtration method, as shown in Figure 2.

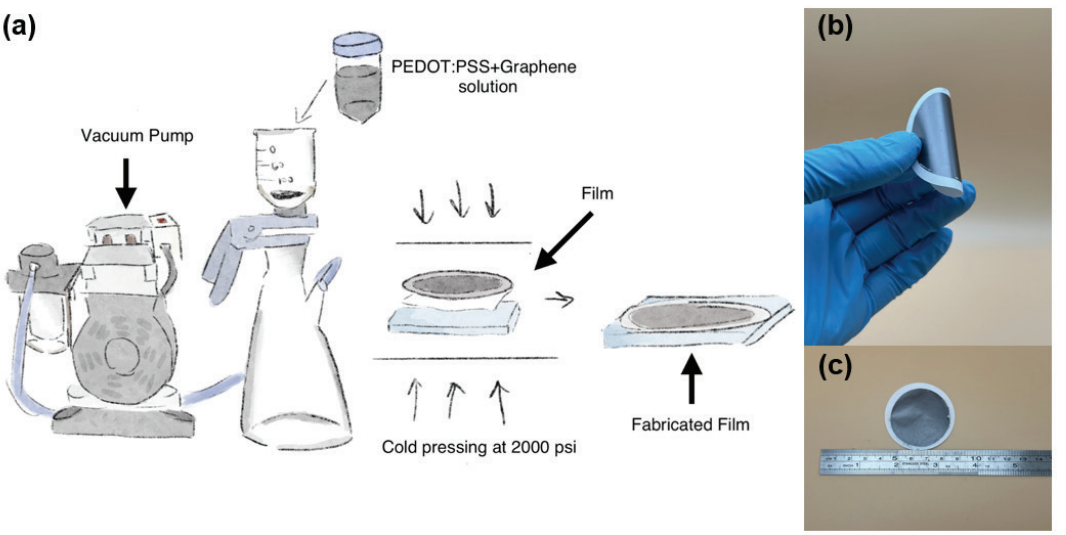

Figure 2. (a) Schematic illustration of the fabrication process using the vacuum-assisted filtration method, and (b, c) fabricated flexible films.

To make TE films, the aqueous dispersion ink materials used in this study were sourced from Sigma-Aldrich (900442). The hybrid ink is dispersed in dimethylformamide with 0.2 mg/mL concentration of PEDOT:PSS and 1 mg/mL exfoliated graphene concentration. PEDOT:PSS is an organic conductive polymer, while graphene is a single layer of carbon atoms arranged in a 2D hexagonal lattice, both known for their excellent thermoelectric properties. The thermoelectric ink was prepared by dispersing 2 mL of a PEDOT:PSS and graphene hybrid solution into 50 mL of deionized water, followed by bath sonication to remove agglomerations. The dispersion was subsequently processed using vacuum filtration, where a vacuum pump drew the solution through a 220 nm pore size membrane (Fisher Scientific; $151 for a pack of 200, or approximately $0.75 per membrane) over several hours. Post-filtration, the films were cold pressed at 2000 psi for 10 minutes to enhance particle packing and promote better charge transport by reducing voids. The final film thickness was primarily governed by the concentration of the hybrid ink, allowing for tunable control over film properties during fabrication.

Figure 2(b) shows the fabricated flexible films with very robust mechanical properties. After fabrication, we used a custom-built setup for measuring room temperature TE properties including electrical conductivity and Sebeck coefficient. TE films were prepared with 23 mm × 3 mm (L×W). We measured three samples for both unsintered and sintered films. Thermal sintering (i.e., annealing) was employed at 120 °C for 30 minutes to investigate the effects of microstructural changes and particle coarsening on the thermoelectric properties of the films.

Figure 3 demonstrates the TE properties measurement setup. After cutting film, they were transferred onto a glass slide as a substrate. ImageJ software was used to measure the width of the samples for accurate electrical conductivity calculation. Then we measured the Seebeck coefficient and electrical conductivity using a developed LabVIEW program. The four-point probe method was used for electrical conductivity measurement. The film is held to a dielectric support substrate with two electrodes through which current I is supplied for electrical conductivity measurement. Two thermocouples are brought into contact with the film and the measurement apparatus placed in air. On the other side of the electrodes are gradient heaters allowing precise control over the temperatures T_h and T_c and thus the temperature gradient $\Delta T = T_h - T_c$. The voltage is measured across the negative leads of the thermocouples. This is done for ten equally spaced currents. The sample resistance R is the slope of the best fit line through the V/I data and the conductivity is then calculated as $\sigma = \frac{L}{RA}$, where L is the distance between the thermocouple tips and A is the cross-sectional area of the sample. The average film thickness of the films was ~5 µm. For Seebeck coefficient measurement, a temperature gradient (~6 K) was applied across the film, and the induced voltage and temperatures were measured using k-type thermocouples (40 gauge). The Seebeck coefficient was calculated as $S = \frac{-\Delta V}{\Delta T}$. The apparatus was calibrated using a standard constantan sample of known properties. The measurement error of the custom-built apparatus was ~5% for both the electrical conductivity and Seebeck coefficient.

RESULTS

The room temperature electrical conductivity and Seebeck coefficient of TE films before and after sintering at 120 ºC are presented in Figure 4. The unsintered TE films showed an average electrical conductivity and Seebeck coefficient of 2373.3 ± 160.8 S/m and -71.1 ± 2.9 µV/K, respectively. This leads to a power factor of 12.03 ± 1.3 µW/mK². In addition, sintering TE films at 120 ºC demonstrates stability of organic thermoelectric films under elevated temperatures. We found that by sintering PEDOT:PSS mixed with graphene nanoplatelets, the electrical conductivity reduces almost 17% whereas Seebeck coefficient remains almost same. This is attributed to reduce carrier concentration or possible

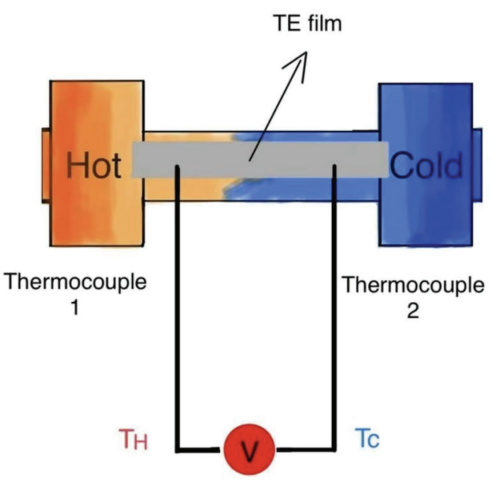

Figure 3. Schematic illustration of room temperature Seebeck coefficient and electrical conductivity measurement setup.

decomposition of PEDOT:PSS could cause reduced charge carrier transport. The power factor of sintered films was 10.17 ± 1.6 μW/mK^2.

To demonstrate the practical application of organic TE materials, a prototype in-plane TE generator was fabricated, as illustrated in Figure 5. The device consisted of five legs composed of PEDOT:PSS mixed with graphene nanoplatelets, each measuring 11 mm × 3 mm (L × W), with a total internal resistance of 537.7 Ω. Device performance was evaluated using a copper plate as a passive heat sink and a commercial heater to establish a controlled temperature gradient, as shown in Figure 5(b). The temperatures at the hot and cold ends were measured using K-type thermocouples connected to a Keysight DAQ970A data acquisition system. After two months of ambient air exposure, the internal resistance increased by only ~1%, indicating strong environmental stability of the fabricated device.

Figure 6 shows the measured device open circuit voltage (V_{oc}) under different temperature gradients up to 15 K. The measured values are almost equal to the theoretical values which are calculated according to the expression V_{oc} =N|S|ΔT where N is the number of TEG legs, S is the Seebeck coefficient, and ΔT is the corresponding temperature gradient with the maximum output voltage of 5.1 mV at ΔT of 15 K.

A detailed cost analysis was conducted based on material prices from commercial suppliers. PEDOT:PSS

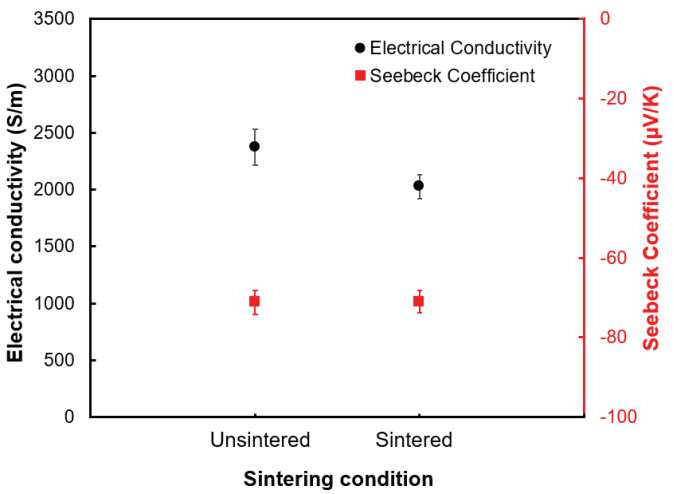

Figure 4. Room temperature thermoelectric properties of fabricated films before and after sintering.

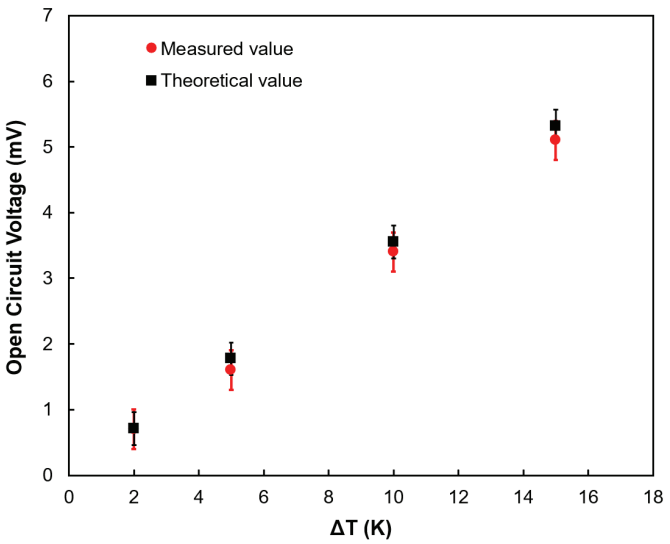

Figure 6. Open circuit voltage of the fabricated TE device.

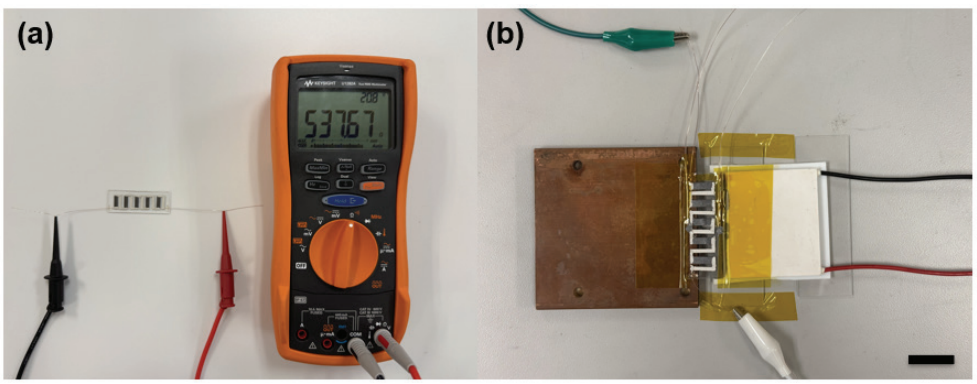

Figure 5. In-plane thermoelectric device made of PEDOT:PSS and graphene. (a) resistance of the device, (b) device performance measurement process. The scale bar is 25 mm.

and graphene, both obtained from Sigma-Aldrich, are priced at $351 for 50 mL. Using 2 mL of this solution diluted in 50 mL of deionized water, the estimated cost per thermoelectric film is approximately $14.04. For a five-leg device (each leg measuring 11 mm × 3 mm), the material cost is calculated at $8.78. When including the filtration membrane—priced at $0.75 per unit—the total cost per device is reduced to just $0.63. Table 1 presents a comprehensive cost breakdown for each component involved in film and device fabrication, providing insight into the economic feasibility of scalable thermoelectric device production.

As demonstrated by these results, flexible organic TE devices, which have been gaining the growing scientific interests, are a promising candidate as renewable energy sources, especially in the application of energy harvesting for flexible and wearable devices based on human body temperature. A new architecture design for conformal thermal contact on the hot surface of heat source is could also enhance thermal transport efficiency and large temperature gradient generation in organic TE devices resulting in higher power outputs.

DISCUSSION

The thermoelectric characterization of PEDOT:PSS/graphene films before and after thermal treatment provides insight into the material's performance and stability. At room temperature, the unsintered films exhibited a high electrical conductivity of 2373.3 ± 160.8 S/m and a Seebeck coefficient of −71.1 ± 2.9 μV/K, resulting in a power factor of 12.03 ± 1.3 μW/mK². Upon sintering at 120 °C, the electrical conductivity decreased by approximately 17%, while the Seebeck coefficient remained largely unchanged. This decline in conductivity is likely due to a reduction in carrier concentration or partial degradation of the PEDOT:PSS structure, which may hinder charge transport. Despite this reduction, the sintered films still demonstrated a solid power factor of 10.17 ± 1.6 μW/mK², indicating their robustness under moderate thermal stress and validating their potential for practical use in thermal environments.

To demonstrate device-level applicability, a flexible in-plane thermoelectric generator was fabricated using five PEDOT:PSS/graphene legs. The prototype had an internal resistance of 537.7 Ω. Testing under applied temperature gradients up to 15 K revealed that the measured open-circuit voltage closely matched theoretical predictions, confirming the reliability of the device's thermoelectric performance. The maximum output voltage reached 5.1 mV, demonstrating the potential of this material system for energy harvesting from low-grade heat sources such as human body. Notably, the device exhibited excellent environmental stability, with only a ~1% increase in internal resistance after two months of air exposure.

A cost analysis further supports the viability of these organic thermoelectric materials for scalable production. With raw materials sourced from commercial suppliers, the estimated cost per film was $14.04, while the cost per five-leg device was $8.78. Including filtration membranes, the total device cost dropped to just $0.63. This cost-efficiency, combined with the film's flexibility, moderate processing conditions, and reliable performance, positions PEDOT:PSS/graphene composites as promising candidates for future applications in flexible and wearable electronics. Future improvements, such as engineering conformal thermal interfaces to enhance heat transfer, could significantly increase the temperature gradient across the device and further boost power output.

CONCLUSION

In conclusion, this study demonstrates the promise of flexible thermoelectric generators based on PEDOT:PSS and graphene as efficient, lightweight, and environmentally friendly energy-harvesting materials. By leveraging the mechanical flexibility and high electrical conductivity of PEDOT:PSS alongside the excellent electrical and

Table 1. Cost analysis of the fabricated TE device

Material/Component	Supplier	Cost	Description
PEDOT:PSS mixed with graphene solution	Sigma-Aldrich	$351 (50 ml)	Concentration: 2 ml in 50 ml of water
Cost per Film	Sigma-Aldrich	$14.04	Based on material usage
Filtration Membrane	Fisher Scientific	$0.63/each	Includes additional fabrication components
Cost per Device	-	$9.38	Device with 5 legs (each leg: 11 mm × 2 mm)

thermal properties of graphene, the fabricated devices exhibit strong thermoelectric performance suitable for applications such as wearable electronics. The use of vacuum filtration enabled the production of uniform, dense films with stable thermoelectric properties. The resulting films achieved a Seebeck coefficient of -71 ± 2.9 μV/K and an electrical conductivity of 2.3×10^3 S/m, yielding a power factor of 12.03 ± 1.3 μW/mK². Sintering at 120 °C caused a slight decrease in electrical conductivity due to changes in microstructure and reduced charge transport. Furthermore, an in-plane prototype device generated a maximum open circuit voltage of 5.1 mV under a ΔT of 15 K. Additionally, a cost analysis supports the economic feasibility of these materials for scalable, sustainable energy applications. This study highlights the potential of organic thermoelectric devices for seamless integration into low-power electronics and wearable technologies.

ACKNOWLEDGMENT

I would like to express my sincere gratitude to Professor Mortaza Saeidi for his invaluable support and insightful guidance throughout this work.

REFERENCES

1. Saeidi-Javash M, Wang K, Zeng M, Luo T, Dowling AW, Zhang Y. Machine Learning-Assisted Ultrafast Flash Sintering of High-Performance and Flexible Silver–Selenide Thermoelectric Devices. *Energy & Environmental Science.* 2022; 15 (12): 5093–5104. https://doi.org/10.1039/D2EE01844F
2. Liang J, Wang T, Qiu P, Yang S, *et al*. Flexible Thermoelectrics: From Silver Chalcogenides to Full-Inorganic Devices. *Energy & Environmental Science.* 2019; 12 (10): 2983–2990. https://doi.org/10.1039/C9EE01777A
3. Gayner C, Kar KK. Recent Advances in Thermoelectric Materials. *Progress in Materials Science.* 2016; 83: 330–382. https://doi.org/10.1016/j.pmatsci.2016.07.002
4. Yang L, Chen Z, Dargusch MS, Zou J. High Performance Thermoelectric Materials: Progress and Their Applications. *Advanced Energy Materials.* 2017; 8 (6). https://doi.org/10.1002/aenm.201701797
5. Dresselhaus MS, Chen G, Tang MY, Yang RG, *et al*. New Directions for Low-dimensional Thermoelectric Materials. *Advanced Materials*. 2007; 19 (8): 1043–1053. https://doi.org/10.1002/adma.200600527
6. Wei J, Yang L, Ma Z, Song P, *et al*. Review of Current High-ZT Thermoelectric Materials. *Journal of Materials Science.* 2020; 55 (27): 12642–12704. https://doi.org/10.1007/s10853-020-04949-0
7. Mukherjee M, Srivastava A, Singh AK. Recent Advances in Designing Thermoelectric Materials. *Journal of Materials Chemistry C*. 2022; 10 (35): 12524–12555. https://doi.org/10.1039/D2TC02448A
8. Russ B, Glaudell A, Urban JJ, Chabinyc ML, Segalman RA. Organic Thermoelectric Materials for Energy Harvesting and Temperature Control. *Nature Reviews Materials.* 2016; 1 (10). https://doi.org/10.1038/natrevmats.2016.50
9. Lee S, Kim S, Pathak A, Tripathi A, *et al*. Y. Recent Progress in Organic Thermoelectric Materials and Devices. *Macromolecular Research*. 2020; 28 (6): 531–552. https://doi.org/10.1007/s13233-020-8116-y, https://doi.org/10.1007/s13233-015-3075-4
10. Ding J, Yamanaka K, Hong S, Chen G, *et al*. Controlling the Thermoelectric Performance of Doped Naphthobisthiadiazole-based Donor–Acceptor Conjugated Polymers through Backbone Engineering. *Advanced Science.* 2024; 11 (48). https://doi.org/10.1002/advs.202410046
11. Hong CT, Kang YH, Ryu J, Cho SY, Jang K-S. Spray-Printed CNT/P3ht Organic Thermoelectric Films and Power Generators. *Journal of Materials Chemistry A*. 2015; 3 (43): 21428–21433. https://doi.org/10.1039/C5TA06096F
12. Mardi S, Yusupov K, Martinez PM, Zakhidov A, Vomiero A, Reale A. Enhanced Thermoelectric Properties of Poly(3-Hexylthiophene) through the Incorporation of Aligned Carbon Nanotube Forest and Chemical Treatments. *ACS Omega*. 2021; 6 (2): 1073–1082. https://doi.org/10.1021/acsomega.0c02663
13. Qian Y, Guo M, Li C, Bi K, Chen Y. New Insight on the Interface between Polythiophene and Semiconductors via Molecular Dynamics Simulations. *ACS Applied Materials & Interfaces.* 2019; 11 (33): 30470–30476. https://doi.org/10.1021/acsami.9b09742
14. Gärisch F, Schröder V, List-Kratochvil EJ, Ligorio G. Scalable Fabrication of Neuromorphic Devices Using Inkjet Printing for the Deposition of Organic Mixed Ionic-electronic Conductor. *Advanced Electronic Materials*. 2024; 10 (12). https://doi.org/10.1002/aelm.202400479
15. Ding J, Liu Z, Zhao W, Jin W, *et al*. Selenium-substituted Diketopyrrolopyrrole Polymer for High-performance P-type Organic Thermoelectric Materials. *Angewandte Chemie International Edition*. 2019; 58 (52): 18994–18999. https://doi.org/10.1002/anie.201911058, https://doi.org/10.1002/anie.201914205
16. Wan C, Gu X, Dang F, Itoh T, *et al*. Flexible N-Type Thermoelectric Materials by Organic Intercalation of Layered Transition Metal Dichalcogenide Tis2. *Nature Materials.* 2015; 14 (6): 622–627. https://doi.org/10.1038/nmat4251
17. Zhang Y, Park S-J. Flexible Organic Thermoelectric Materials and Devices for Wearable Green Energy

Harvesting. *Polymers.* 2019; 11 (5): 909. https://doi.org/10.3390/polym11050909

18. Chauhan A, Kumar S, Satapathy DK, Battabyal M. Polymer-Infused Textile Thermoelectrics for Power Generation. *ACS Applied Electronic Materials*. 2024; 6 (4): 2774–2781. https://doi.org/10.1021/acsaelm.4c00352
19. Insawang M, Vora-ud A, Seetawan T, Muntini MS, Phan TB, Kumar M. Enhancing Thermoelectric Power Factor of PEDOT:PSS/SNSE2 Nanocomposite Sheets by Rapid Thermal Annealing. *Journal of Electronic Materials.* 2024; 54 (5): 3494–3500. https://doi.org/10.1007/s11664-024-11687-5
20. Lang U, Naujoks N, Dual J. Mechanical Characterization of Pedot:PSS Thin Films. *Synthetic Metals.* 2009; 159 (5–6): 473–479. https://doi.org/10.1016/j.synthmet.2008.11.005
21. Geim AK. Graphene: Status and Prospects. *Science.* 2009; 324 (5934): 1530–1534. https://doi.org/10.1126/science.1158877
22. Perreault F, Fonseca de Faria A, Elimelech M. Environmental Applications of Graphene-Based Nanomaterials. *Chemical Society Reviews.* 2015; 44 (16): 5861–5896. https://doi.org/10.1039/C5CS00021A
23. Olabi AG, Abdelkareem MA, Wilberforce T, Sayed ET. Application of Graphene in Energy Storage Device – A Review. *Renewable and Sustainable Energy Reviews.* 2021; 135: 110026. https://doi.org/10.1016/j.rser.2020.110026
24. Khan U, O'Neill A, Lotya M, De S, Coleman JN. High-concentration Solvent Exfoliation of Graphene. *Small.* 2010; 6 (7): 864–871. https://doi.org/10.1002/smll.200902066
25. Sahoo NG, Pan Y, Li L, Chan SH. Graphene-based Materials for Energy Conversion. *Advanced Materials.* 2012; 24 (30): 4203–4210. https://doi.org/10.1002/adma.201104971